Research Square

Preprints are preliminary reports that have not undergone peer review.
They should not be considered conclusive, used to inform clinical practice,
or referenced by the media as validated information.

Transcriptome and metabolome analysis reveals mechanism of light intensity modulating iridoids biosynthesis in Gentiana macrophylla Pall.

Huanhuan Fu

1464741616@qq.com

Shaanxi University of Chinese Medicine https://orcid.org/0000-0002-5765-9485

Yaomin Wang

Shaanxi University of Chinese Medicine

Fakai Mi

Qinghai Normal University

Li Wang

Shaanxi University of Chinese Medicine

Ye Yang

Shaanxi University of Chinese Medicine

Fang Wang

Shaanxi University of Chinese Medicine

Zhenggang Yue

Shaanxi University of Chinese Medicine https://orcid.org/0000-0001-6296-8509

Yihan He

Shaanxi University of Chinese Medicine

Research Article

Keywords: Gentiana macrophylla Pall., Transcriptome analysis, Metabolome analysis, Light intensity, Iridoid biosynthesis

Posted Date: January 15th, 2024

DOI: https://doi.org/10.21203/rs.3.rs-3849087/v1

License: This work is licensed under a Creative Commons Attribution 4.0 International License.
Read Full License

Version of Record: A version of this preprint was published at BMC Plant Biology on June 11th, 2024. See the published version at https://doi.org/10.1186/s12870-024-05217-y.

Abstract

Light intensity is a key factor affecting the synthesis of secondary metabolites in plants. However, the response mechanism of metabolites and genes in *G. macrophylla* under different light intensities have not been determined. In the present study, *G. macrophylla* seedlings were treated with LED light intensities at 15 μmol/m^2/s (low light, LL), 90 μmol/m^2/s (medium light, ML) and 200 μmol/m^2/s (high light, HL), and the leaves were collected at 5-day for further investigation. A total of 2162 metabolites were detected, in which, the abundant metabolites were identified as flavonoids, carbohydrates, terpenoids and amino acids. A total of 3313 and 613 differential expression genes (DEGs) were identified after HL and LL groups, respectively, compared to the ML group, enriched in KEGG pathways such as carotenoid biosynthesis, carbon metabolism, glycolysis/gluconeogenesis, amino acids biosynthesis, plant MAPK pathway and plant hormone signaling. In which, the transcription factors *GmMYB5* and *GmbHLH20* were found to be significantly correlated with loganic acid biosynthesis; the expression of photosystem-related enzyme genes was changed under different light intensities, regulating the expression of enzyme genes involved in the carotenoid, chlorophyll, glycolysis and amino acids pathway and thus affecting their metabolic biosynthesis. As a result, low light inhibited photosynthesis, thus, delaying glycolysis, accumulating certain amino acids and decreasing loganic acid production, while high light got an opposite trend. Our research contributed significantly to understanding the molecular mechanism of light intensity in controlling metabolic accumulation in *G. macrophylla*.

Key Message

Light intensity regulated photosynthesis rates, then modulated primary and secondary metabolic pathways, key responsive TFs and light related hormones signaling, hence affected iridoids accumulation in *Gentiana macrophylla*.

Introduction

Gentiana macrophylla Pall. (Gentianaceae) is an important herbal medicine with a variety of pharmacological activities (Peng and Ai 2021). Its major secondary metabolites are iridoids, the main components as loganic acid, swertiamarin, gentiopicroside and sweroside (Cao and Wang 2010), showing antidiabetic (Hao, et al. 2023; Liu, et al. 2023), anti-proliferative (Yoshikawa, et al. 2022), hepatoprotective, anti-inflammatory (Usmanov, et al. 2023), antioxidant (Zhang, et al. 2023) and neuroprotective properties (Zengin, et al. 2023). The resource of *G. macrophylla* is distributed widely in almost all regions of northern China, across 33°N ~ 53°N, 103°E ~ 135°E, and altitudes ranging from 400 to 2400 m. Due to the complex distribution of the natural environment, the quality of herbal materials is extremely varied. Although several researchers have observed ecological factors affecting *G. macrophylla* to generate differential secondary metabolite contents (Li, et al. 2016), the underlying mechanism needs to be further explored.

Light, as one of the most important ecological factors, has been observed to affect plant growth and development, and revealed to regulate the production of secondary metabolites in medicinal plants under different light-emitting diodes (LEDs) or other light sources (Chen, et al. 2018). Three light environment factors: light intensity, light quality and photoperiod (Xie, et al. 2022) were always investigated during the research procedure. For example, after treatment with different light qualities and intensities, the biomass production of *Hypericum perforatum* roots increased in cultures grown under dark and red light (Ahmad, et al. 2019). The beneficial glucosinolate glucoraphanin and the anti-nutritional glucosinolate progoitrin in Chinese cabbage plantlets were synthesized at light intensities of 200 and 50 μmol/m^2/s, respectively (Zhou, et al. 2023). Treated with different light intensities (natural light, shade rate 50%, shade rate 70%, and shade rate 90%), the contents of chlorophyll a (Chl a), Chl b, Chl a + b, and Chl a/b in *Angelica dahurica* enhanced, while the ratio of Chl a/b reduced with increasing shade (Huang, et al. 2022). Moreover, the content of saponarin in Barley Sprouts was decreased along with reducing light intensity (Yoon, et al. 2023). The content of total sesquiterpenoid was highest in the rhizome of *Atractylodes lancea* under 80% mild shading compared with 100% strong light and 7% low light (Guo, et al. 2022a). 23 terpenoids derivatives were identified in the leaves of *Pinus massoniana*, and most of which were decreased under low light treatment (Shi, et al. 2022). The synthesis of monoterpene in *Lilium* 'Siberia' was increased under light intensities of 200 and 600 μmol/m^2/s (Yang, et al. 2023). The content of anthocyanin in blueberry fruits increased by a factor of 1.76 to 24.13 at 100% light intensity compared with the non-full light (Han, et al. 2023).

The photoregulation mechanism was also be explored. Higher altitude with strong light intensity, increased the expression of genes involved in light stress (*HSP18.1*, *HSP70*, *UBC4*, *ERF5*, *ERF9*, *APX3* and *EX2*) and genes involved in flavonoid biosynthesis (*PAL*, *CHS1*, *IFRL*, *ANS*, *MYB4*, *bHLH137*, *CYP6*, *PPO1* and *ABCB19*), thus promoting the accumulation of flavonoids, flavonols, and anthocyanins in *Sinopodophyllum hexandrum* (Zhao, et al. 2023). Four key genes in anthocyanin biosynthesis pathway (*CHI*, *DFR*, and *ANS*) and 147 transcription factors (MYB, bHLH, bZIP, ERF, and NAC) involved in malonylshisonin biosynthesis have been identified (Xie, et al. 2022). In *Angelica dahurica*, under 90% natural light, coumarin biosynthesis may be decreased by reducing the expression of *COMT* and *4CL* genes (Huang, et al. 2022). Thus, the results of previous studies indicated that light might act directly on photoregulatory genes, and subsequently affect critical genes in the secondary metabolite biosynthesis, hence activating or inhibiting metabolite accumulation in plant tissues.

In our study, the mechanism of iridoid metabolites as the key active ingredients in *G. macrophylla* leaves in respond to light intensity was studied. The *G. macrophylla* seedlings were treated with different light intensities, and then variation analysis of metabolites levels and their regulator genes levels were detected by metabolome and transcriptome; correlation analysis between metabolites and transcription factors (TFs) and correlation analysis between differential TFs and metabolites regulator genes involved in iridoid biosynthesis were performed. The results showed that light modulated the iridoid biosynthesis in *G. macrophylla*, and the mechanism was revealed as different light intensities altering the photosynthesis rate, successively regulating the primary metabolic system, the secondary metabolic

pathway, the key responsive TFs and the light related hormone signaling, hence increasing or decreasing the accumulation of iridoids. This study provides new insights into the molecular mechanism underlying the biosynthesis and regulation of iridoids in *G. macrophylla*.

MATERIALs AND METHODS

Plant Materials and Treatments

G. macrophylla seedlings were grown for 12 h under illumination a day, at 26 ± 1 1°C and 68% humidity in the laboratory. At the six-leaf stage (grown for 6 months), seedlings were exposed to light at different intensities: the photosynthetic photon flux density (PPFD) of the LED lights was set at 15 μmol/m^2/s (low light, LL), 90 μmol/m^2/s (medium light, ML) or 200 μmol/m^2/s (high light, HL), with a photoperiod of 14 h light and 10 h dark (day/night conditions), at 26 ± 1°C and 68% humidity in the laboratory. Five-day-old samples were collected for further analysis. Leaves of the three treatments samples were collected: one portion was immediately frozen in liquid nitrogen and stored at -80°C for metabolomic and transcriptomic analysis as well as RNA extraction, while another portion was used to determine the contents of secondary metabolites.

The contents determination of Chls and carotenoids

For each sample, 0.1 g of fresh leaf sample was extracted in 5 mL of 95% ethanol, then 200 μL extraction solution were added to a 96-well plate and the absorbance values (A) were measured at wavelengths of 665 nm, 649 nm and 470 nm in a microplate reader. The content of Chl was calculated as Chl = Chl a + Chl b, Chl a = (13.95 × A_{665} − 6.88 × A_{649}) V/1000 × W, and Chl b = (24.69 × A_{649} − 7.32 × A_{665}) V/1000 × W. The content of carotenoids was calculated as carotenoids = (1000 × A_{470} − 2.05 × Ca − 114.8 × Cb)/(245 × 1000 × W) (Guo, et al. 2022b). The results are expressed in mg/g, in which, Ca is the concentration of Chla, Cb is the concentration of Chl b, V is the volume of the extract, and W is the fresh leaf weight.

The content determination of the secondary metabolites

For each sample, 20 mg of dry weight sample was extracted in 1 mL methanol via ultrasonication for 3 times, each time for 40 min; centrifuged for 5 min at 12000 rpm, and the liquid supernatant was merged and filtered using a 0.22 μm membrane. The contents of four major iridoid metabolites, loganic acid, sweroside, swertiamarin and gentiopicroside, were determined *via* LC-20ADXR HPLC (Shimadzu, Japan) (Welch 4.6 mm × 250 mm, C18 5 μm particles (Welch, China); UV detector, 254 nm; column temperature, 30°C; flow rate, 0.8 mL/min), using gradient solvent system ACN (Welch, China)/H_2O (with 10% phosphoric acid) as the mobile 0–35 min, ACN 10%. Each injection volume was set at 10 μL.

The standard curve was constructed from the metabolite content (*X*, mg/mL) and peak area (*Y*). The linear regression equation was $Y = 1{,}602{,}377.2743\ X + 7{,}867.6622$ (linear range 0.00214814 mg/mL – 1.1 mg/mL) for loganin acid, $Y = 2{,}933{,}123.5429\ X + 108.4713$ (linear range, 0.0158 mg/mL – 1.0112

mg/mL) for sweroside, $Y = 3{,}930{,}675.6374\ X - 5{,}906.8466$ (linear range, 0.03225 mg/mL – 4.128 mg/mL) for gentiopicroside, $Y = 18{,}813{,}950.6495\ X + 12{,}425.4530$ (linear range, 0.0009875 mg/mL – 1.0112 mg/mL) for swertiamarin. Each group was repeated 3 times.

Transcriptome analysis of differentially expressed genes (DEGs)

Transcriptome sequencing was performed by Beijing Genomics Institute (BGI) (Shenzhen, China) (https://www.genomics.cn/). The *G. macrophylla* reference genome was obtained from the following link (https://www.ncbi.nlm.nih.gov/assembly/GCA_026214975.1) (Zhou, et al. 2022). The HISAT2 software (version 2.0.1) (Kim, et al. 2015) was used for alignment to map the filtered reads to the reference genome. Differential analysis of three groups was performed using DESeq2 (Love, et al. 2014) to identify DEGs. The false discovery rate (FDR) correction *p*-value was calculated using the Benjamini-Hochberg method, and DEGs were identified according to FDR ≤ 0.05 and |log2 fold change| ≥ 1.0 (Shao, et al. 2022).

National Center for Biotechnology Information (NCBI), Non-redundant (Nr, http://ftp.ncbi.nih.gov/blast/db/FASTA/nr.gz), Kyoto Encyclopedia of Genes and Genomes (KEGG, https://www.kegg.jp/), and Gene Ontology (GO, http://geneontology.org/) databases were used for gene function annotation. DEGs were functionally classified by GO and KEGG annotation, the phyper function of the *R* software was used for enrichment analysis, and FDR ≤ 0.05 were considered as significant enrichment. The correlations of differential genes, differential TFs and metabolites were analysed and heatmaps were drawn in with metware cloud (https://cloud.metware.cn/#/home), and the network diagram was drawn by Cytoscape.

LC-MS analysis of metabolite profiles

Metabolite profiling was conducted using an untargeted metabolome method at BGI (Shenzhen, China) (https://www.genomics.cn/). For each sample, 50 μg of the samples was weighted into 1.5 mL Eppendorf tubes and soaked in 800 μL of pre-cooled extraction solution (MeOH : H_2O = 7 : 3, v/v) along with 20 μL of internal standard. The mixture was homogenized using a weaving grinder at 50 Hz for 10 minutes, followed by ultrasonication in a water bath at 4°C for 30 minutes. After standing for 1 hour at -20°C, the extracts were centrifuged at 14000 rpm at 4°C for 15 minutes. 600 μL supernatant was filtered using a 0.22 μm membrane. Additionally, 20 μL of filtered solution from each sample was combined to create a mixed QC sample, which was used to access the repeatability and stability of the LC/MS analysis. Data preprocessing was performed using metaX (Wen, et al. 2017) to obtain all forms of compounds and their corresponding intensities for subsequent data analysis. Differential metabolites were identified using thresholds of variable significance of *p*-value ≤ 0.5 and fold change ≥ 2 or ≤ 0.5.

Classification and functional annotation analysis were performed to obtain KEGG ID, category, and KEGG pathway of the identified metabolites, compared with KEGG and HMDB database.

Genes expression analysis by RT-qPCR

Total RNA was isolated using the Polysaccharide Polyphenol Plant Total RNA Extraction Kit (Bioteke, Beijing). The concentration and purity of RNA were detected by Nanodrop (Thermo Fisher, USA) and RNA integrity was detected by 1% agarose gel electrophoresis (Solarbio, Beijing), followed by cDNA synthesis using the PrimeScript™ IV 1st Strand cDNA Synthesis Mix (TaKaRa, Dalian), and stored at -20°C. RT-qPCR was performed using the qTOWER 2.0 system (Analytik Jena, Germany) under the cycling conditions: 95°C for 30 s; 95°C for 5 s and 60°C for 20 s, 40 cycles. The relative expression of the genes was calculated by $2^{-\Delta\Delta Ct}$ method. The *SAND1* gene was used as an internal reference (He, et al. 2016). Each group was repeated 3 times. The NCBI website (https://www.ncbi.nlm.nih.gov/tools/primer-blast/index.cgi?LINK_LOC=BlastHome) was used to design the primers for the target genes (Supplementary Table 1).

Statistical analysis

Statistical analysis of data was conducted using Excel, and the results were presented as means ± *SD*. Graph Pad Prism 8.0 software was used for data visualization, and different treatment groups were analysed using *t*-test. $P \leq 0.05$ was considered to be statistically significant.

Results

Compared with HL and ML groups, the plant morphology of seedlings under low light intensity, was present different growth trend: on the 5th day, the apical leaves appeared clear phototaxis, while, with the time going, all leaves turned yellow and gradually blighted (Fig. 1). Considering the status of the leaf growth and the plant integrity, the 5-day-old samples were collected for further analysis.

The variation of Chls and carotenoids contents at different light intensities

Chls and carotenoids are two kinds of products produced during photosynthesis, and their contents can represent the photosynthetic intensity. As shown in Fig. 2, the contents of Chl and carotenoids were gradually increased along with the intensity of light, suggesting our model was suitable for studying the influence of different light intensities on the growth and development of *G. macrophylla*.

The effect of different light intensities on the contents of iridoid metabolites

As loganic acid, swertiamarin, gentiopicroside and sweroside are four major active components, their contents could represent the degree of metabolites accumulation during the growth and development of *G. macrophylla*. The results showed that, compared HL to ML group, all four components exhibited a significant increasing trend as the contents of loganic acid, swertiamarin, gentiopicroside and sweroside increased by 49.44%, 30.54%, 14.67% and 40.94%, respectively; compared LL to ML group, the accumulation of loganic acid and swertiamarin *vs* gentiopicroside and sweroside indicated converse

trends as the contents of loganic acid and swertiamarin were decreased by 72.39% and 2.21%, respectively, and the contents of gentiopicroside and sweroside were increased by 19.77% and 49.62% respectively (Fig. 3b). These results suggested that under low light intensity treatment, self-protection function in plants was triggered, thus some metabolites crucial for the growth and development as gentiopicroside and sweroside in *G. macrophylla*, may be produced responded to external stimulus.

Metabolomic analysis of metabolites at different light intensities

As shown in Fig. 4a, a total of 2162 metabolites were identified by untarget metabolome analysis, and categorized into 38 classes according to their structural features, including flavonoids (139, comprising 6.43%), terpenoids (135, comprising 6.24%), lipids (115, comprising 5.32%), benzene and derivatives (72, comprising 3.33%), phenylpropanoids (51, comprising 2.36%), phenols and derivatives (48, comprising 2.22%), carbohydrates (25, comprising 1.16%), amino acids, peptides, and analogues (23, comprising 1.06%), alkaloids (20, comprising 0.93%), organic acids (17, comprising 0.79%), other compound types, and unknown classification (1319, comprising 61.01%). Among them, 32 iridoid metabolites were identified, including 7 secoiridoids as gentiopicroside, swertiamarin, sweroside, loganic acid, loganin, secoxyloganin and 6-hydroxysweroside (Fig. 4b). Moreover, the variations in the contents of loganic acid, swertiamarin, gentiopicroside, loganin, and sweroside were largely consistent with the HPLC determined results (Fig. 3b).

Differentially expressed metabolites (DEMs) between pairs of samples (ML *vs* LL group, ML *vs* HL group, and LL *vs* HL group) were determined on the basis of variable significance with a p-value ≤ 0.05 and a fold change ≤ 0.5 or ≥ 2. Thus, DEMs of 307, 156 and 405 in ML *vs* LL group, ML *vs* HL, and LL *vs* HL group were distinguished, respectively, in which, the numbers of upregulated DEMs were 155, 79 and 202, while the numbers of downregulated DEMs were 152, 77 and 203, respectively (Fig. 5a). Besides, 14 metabolites were expressed differentially in all three comparison groups, including 1 carbohydrate (sucrose), 1 amino acid (L-histidine), 1 fungal toxin (aflatoxin G2), 2 organic acids (N6, N6, N6-trimethyl-L-lysine and aspartame), and the remainder were classified as unknown (Fig. 5b).

Among the total 544 DEMs, 70 compounds mainly as flavonoids, carbohydrates, terpenoids, and amino acid compounds (Fig. 6), were enriched in KEGG pathways such as metabolic pathway, aminoacyl-tRNA biosynthesis, secondary metabolite biosynthesis, amino acids biosynthesis, and ABC transporters (Fig. 5c-e). In addition, after clustering analysis, they were roughly divided into two branches, significantly responding to light intensity (Fig. 6, Supplementary Table 2). Thus, the results indicated that light intensity regulated the metabolites biosynthesis in *G. macrophylla*, *via* influencing the function of carbon metabolism, glycolysis/gluconeogenesis, plant hormone signal transduction, and photosynthesis.

Transcriptomic analysis of differentially expressed genes (DEGs) at different light intensities

A total of 9 group samples collected in 5-day were performed transcriptome sequencing, and 24.32 GB of clean data (GC content ranging from 42.97–43.42%) within each sample exceeding 2.5 GB were acquired, in which, the Q30 base percentage for each library was ≥ 91.75% was considered to be high quality reads for further analysis. In addition, more than 95% of the clean reads could be mapped to the reference genome (Supplementary Table 3).

GO enrichment analysis

A total of 3313, 673 and 7758 numbers of DEGs in ML *vs* LL, ML *vs* HL, and LL *vs* HL group were obtained, respectively (Fig. 7a). After GO enrichment analysis was performed, only 2432, 436 and 5410 numbers of DEGs were enriched in the respective groups, primarily grouped into three main categories: biological processes, molecular functions, and cellular components. Furthermore, in each comparable group, the three categories were subdivided into 37, 31 and 38 smaller numbers of functional categories, respectively (Fig. 7b-d). The TOP20 categories (the final 20 ones with the lowest FDR values) were selected for GO enrichment analysis (Fig. 7e-g).

GO enrichment analysis of ML *vs* LL group revealed that DEGs were particularly enriched in organelles and cell membranes such as plastid, chloroplast, thylakoid, plastid membrane, and photosynthetic membrane of the cellular components category; DEGs were mainly associated with photosynthesis, including both photosynthesis and photosynthesis light harvesting of the biological processes category; DEGs were notably enriched in enzyme activity and catalytic activity, encompassing oxidoreductase activity, carbohydrate phosphatase activity, catalytic activity and sugar phosphatase activity of the molecular functions category (Fig. 7e).

GO enrichment analysis of ML *vs* HL group revealed that DEGs were significantly enriched in metabolic processes, signal transductions, defense reactions such as response to stimulus, phenylpropanoid biosynthesis process, lignin biosynthesis process, secondary metabolite biosynthesis process, signal transduction, signaling and secondary metabolic process of the biological processes category; DEGs were notably enriched in enzyme activities and bindings such as oxidoreductase activity, anion binding, ribonucleotide binding, small molecule binding and carbohydrate derivative binding of the molecular functions category (Fig. 7f).

GO enrichment analysis of LL *vs* HL group revealed that DEGs were significantly enriched in organelles, cell membranes and cytoplasm such as plastid, chloroplast, thylakoid, envelope and the cytoplasm of the cellular components category; DEGs were mainly enriched in plastid organizations and metabolic processes, such as small molecule metabolic process, plastid organization, carbohydrate metabolic process, oxoacid metabolic process, carboxylic acid metabolic process, and organic acid metabolic process of the biological processes category; DEGs were notably enriched in enzyme activities and bindings such as oxidoreductase activity, small molecule binding, and anion binding of the molecular functions category (Fig. 7g).

KEGG analysis

A total of 1619 numbers of annotated genes were associated with 132 numbers of KEGG pathways in ML *vs* LL group, in which 19 KEGG pathways were present differential (FDR < 0.05) (Fig. 7h), such as carotenoid biosynthesis (ko00906), carbon metabolism (ko01200), glycolysis/gluconeogenesis (ko00010), carbon fixation in photosynthetic organisms (ko00710), biosynthesis of amino acids (ko01230), terpenoid backbone biosynthesis (ko00900), tryptophan metabolism (ko00380), biosynthesis of cofactors (ko01240), and pyruvate metabolism (ko00620).

A total of 321 numbers of annotated genes were associated with 101 numbers of KEGG pathways in ML *vs* HL group, in which 4 KEGG pathways were present differential (Fig. 7i), such as alpha-linolenic acid metabolism (ko00592), MAPK signaling pathway-plant (ko04016), plant hormone signal transduction (ko04075), plant-pathogen interaction (ko04626) and monoterpenoid biosynthesis (ko00902).

A total of 3955 numbers of annotated genes were associated with 137 numbers of KEGG pathways in LL *vs* HL comparison, in which 34 KEGG pathways were present differential (Fig. 7j), such as photosynthesis-antenna proteins (ko00196), carotenoid biosynthesis (ko00906), carbon metabolism (ko01200), biosynthesis of amino acids (ko01230), glycolysis/gluconeogenesis (ko00010), pentose phosphate pathway (ko00030), glycerophospholipid metabolism (ko00564), glycerolipid metabolism (ko00561), biosynthesis of cofactors (ko01240), carbon fixation in photosynthetic organisms (ko00710) and terpenoid backbone biosynthesis (ko00900).

Identification of DEGs related to the iridoid biosynthesis pathway

As mentioned above, iridoid metabolites were the major active components in *G. macrophylla*, and the genes related to the iridoid biosynthesis pathway in DEGs were chosen for further analysis. A total of 38, 6, and 61 numbers of DEGs, belonging to 23 gene families, were revealed relating to the iridoid biosynthesis pathway in ML *vs* LL, ML *vs* HL, and LL *vs* HL group, respectively (Fig. 8b). These gene families were illustrated as *GmDXS*, *GmDXR*, *GmCMS*, *GmCMK*, *GmMCS*, *GmHDR*, *GmHDS*, *GmIDI*, *GmHMGS*, *GmHMGR*, *GmMK*, *GmPMK*, *GmGPPS*, *GmGGPPS*, *GmGES*, *GmG10H*, *Gm8-HGO*, *GmIS*, *GmIO*, *Gm7-DLGT*, *Gm7-DLNGT*, *Gm7-DLH*, and *GmSLS* (Supplementary Table 4). To visualize the changes in pathway DEGs in *G. macrophylla* leaves under different light intensities treatments, we produced a heatmap (Fig. 8a). The results showed that under low light conditions, the expression of most genes in iridoid biosynthesis pathway was downregulated, including the upstream genes as *GmHMGS*, *GmHMGR*, *GmMK* and *GmPMK* in the MVA pathway and *GmDXS*, *GmDXR*, *GmCMS*, *GmCMK*, *GmMCS*, *GmHDS*, *GmHDR*, *GmIDI* in the MEP pathway, as well as the downstream enzyme genes *GmGPPS*, *GmGES*, *GmG10H*, *Gm8-HGO, GmIS*, *GmIO*, *Gm7-DLNGT*, *Gm7-DLH* and *GmSLS* in the iridoid backbone biosynthesis pathway. On contrary, after exposure to high light intensity, the expression of most genes was upregulated. Accordingly, two inferences were obtained, one was that light intensity affected the expression on both of the upstream and downstream genes related to iridoid biosynthesis; the other was that the MEP pathway was primary with a greater number of DEGs compared with MVA pathway.

Identification and analysis of TFs in respond to light intensity

A total of 1395 TFs in *G. macrophylla*, classified into 50 TF families, were identified on the basis of online data from PlantTFDB. Among these TF families, the most abundant were MYB (144 entries), AP2-EREBP (93 entries), bHLH (68 entries), NAC (55 entries) and WRKY (70 entries) (Fig. 9a). In particular, 2 TFs expressed differentially across all three comparison groups, one entry was designated as *GmbHLH20* of the bHLH family, and the other entry was designated as *GmMYB5* of the MYB family (Fig. 9b).

Correlation analysis of TFs, metabolites and genes related to iridoid synthesis

GmbHLH20 was revealed to regulate positively in the biosynthesis of loganic acid, while *GmMYB5* was negative ones, on basis of correlation analysis (Pearson, $R > 0.8$) between differential TFs and iridoid metabolites (Fig. 9c). Then, correlation analysis of *GmbHLH20*, *GmMYB5* and the iridoid biosynthesis genes was performed. The results showed, *GmbHLH20* was present a negative correlation with *GmMYB5* (Fig. 9d); *GmbHLH20* might positively regulate the expression of *GmDXS1*, *GmDXS2*, *GmHDR1*, *GmHDR2*, *GmGES*, *GmG10H3*, *Gm8-HGO1*, *Gm8-HGO3*, *Gm8-HGO6*, *Gm8-HGO7*, *GmIS3*, *GmIO1*, *Gm7-DLH4* and *GmGGPPS6*, while negatively regulate the expression of *GmHMGR2*, *GmG10H1*and *Gm7-DLNGT3*; *GmMYB5* might positively regulate the expression of *GmHMGR1*, *GmHMGR2*, *GmG10H1* and *Gm7-DLNGT3*, while negatively regulate the expression of *Gm 8-HGO7*. Accordingly, an inference was obtained that *GmbHLH20* and *GmMYB5* may play key roles in the light response and the regulation of iridoids.

RT-qPCR analysis of DEGs in fresh leaves of G. macrophylla seedlings compared to RNA-seq

RT-qPCR was performed to analyse the DEGs associated with iridoid synthesis, including two candidate genes as *GmbHLH20* and *GmMYB5*, and 22 key genes in the iridoid pathway as *GmDXS*, *GmDXR*, *GmCMS*, *GmMCS*, *GmHDR*, *GmHDS*, *GmHMGS*, *GmHMGR*, *GmMK*, *GmPMK*, *GmIDI*, *GmGGPPS*, *GmGES*, *GmG10H*, *Gm8-HGO3*, *Gm8-HGO6*, *GmIS*, *GmIO*, *Gm7-DLGT*, *Gm7-DLNGT*, *Gm7-DLH* and *GmSLS*. As shown in Fig. 11, *GmbHLH20* as a positive TF regulator and most genes in the iridoid pathway showed an upward or downward trend in expression under high or low light intensity, respectively; while *GmMYB5* as a negative TF regulator displayed contrary tendency. Notably, the transcript profiles of all selected genes were highly consistent with those obtained from the RNA-seq data (Fig. 10).

Discussion

Unlike animals, the plants are one species unable to move away from their native-born place, face differential ecological factors, thus passively accept the environmental stimuli (Goh, et al. 2003). To adapt to the external environment, plants initiate internal regulation, producing metabolites to benefit the growth and development, or to defend themselves. Many studies have revealed the metabolites

accumulation was affected by the ecological factors (Li, et al. 2016). For *G. macrophylla*, intricate ecological conditions, such as various distribution, temperature, altitude, light and moisture, have been observed to influence the contents of iridoid metabolites (Cao and Wang 2010; Lu, et al. 2016; Wu, et al. 2009), however, complex mechanisms have not yet been revealed. Thus, the herbal materials from different habitats were present difference in quality, unfavorable for clinical application.

Among the ecological factors, light is considered to be essential. LED light sources of different intensities have been found to have distinct effects on the plant growth (Proietti, et al. 2023; Shang, et al. 2023), the protective enzyme system (Gong, et al. 2023), the photosynthesis (Yoon, et al. 2023), and the accumulation of secondary metabolites (Barh, et al. 2022; Li, et al. 2022; Yoon, et al. 2023). Photosynthesis plays a vital role in oxidation respiratory chain, as the primary driving force to initiate alteration during the growth and development of plants. Within the photosynthetic system, accessory pigments such as various Chls, carotenoids, and phycobilins, serving as energy receptors, absorb the energy from photons and channel it towards the primary reaction centers named as P680 in photosystem II and P700 in photosystem I for further photochemical processes (HÄDer 2022). In this study, both Chls and carotenoids exhibited increased expression along with the increasing of light intensity (15, 90 and 200 μmol/m^2/s) (Fig. 2a and b), as well the expression of enzyme genes related to the synthesis of phytoene, lycopene, carotene, zeaxanthin, violaxanthin, and xanthoxin in the carotenoid biosynthesis pathway (map00906), and Chl a and Chl b in the porphyrin metabolism pathway (map00860) also displayed the same expression trend (Supplementary Fig. 1–4, Supplementary Tables 5 and 6) in the KEGG differential genes enrichment analysis. Furthermore, with the prolongation of the light treatment duration, the leaves of *G. macrophylla* seedlings under low light gradually turned yellow and wilted during the 15 days period, deduced as a gradual loss of Chls leading to impaired photosynthesis. Thus, subsequent biochemical reactions would be triggered due to the alteration of photosynthesis.

The first consequence is that the impaired photosynthetic carbon assimilation would affect the primary metabolic pathways in plants, including amino acid metabolism, starch and sucrose metabolism (Zhang, et al. 2017). When *G. macrophylla* was exposed to different light intensities, the levels of certain amino acids and their derivatives (L-glutamic acid, L-leucine, L-tyrosine, D-glutamic acid, L-phenylalanine, L-histidine, and asparagine) were present higher expression in LL group compared to ML and HL groups, as well the expression of enzyme genes involved in the pathway reflected same trend (Supplementary Figs. 5 and 6, Supplementary Table 7). These findings were in accordance with recent research conclusion that the levels of some amino acids such as phenylalanine and tryptophan in plants, were commonly upregulated under diverse environmental conditions, such as hydropenia, cold stress and during dark-induced senescence (Gad, et al. 2016). However, levels of maltotriose, d-raffinose, sucrose, and lactose, were present lower expression in LL groups, as well as the expression of genes in the glycolysis, the pentose phosphate pathway, and the shikimate pathway (Supplementary Fig. 6). It is easily to understand that increased rate of photosynthetic activity brings out a reduction in the efficiency of converting light energy into chemical energy, thus the carbohydrate stores are depleted under low light intensity, however, for survival, vital substances such as amino acids in plants were accumulated primarily (Supplementary Fig. 5) (Kc, et al. 2021).

The second consequence is that deferred glycolysis/gluconeogenesis by the impaired photosynthetic carbon assimilation, would affect the secondary metabolites pathway in plants (Yoon, et al. 2023). So far, the biosynthesis pathway of iridoid metabolites was partly revealed as initiating from MVA or MEP pathway to generate IPP and GPPS, then, under the geranyl diphosphate synthase *GES*, geraniol 8-hydroxylase *G10H*, 8-hydroxygeraniol dehydrogenase *8-HGO*, (S)-8-oxocitronellyl enol synthase *IS*, 7-deoxyloganetic acid glucosyltransferase *7-DLGT*, and 7-deoxyloganate 7-hydroxylase *7-DLH* to successively catalytic generate geraniol, 8-hydroxygeraniol, 8-oxogeranial, 7-deoxyloganetic acid, 7-deoxyloganic acid and loganic acid, and finally under secologanin synthase *SLS* to secologanate (Hu, et al. 2022). In this study, the levels of the mevalonic acid content along with expression of the key genes in MVA pathways, as well as genes expression in MEP pathway, were present lower in LL group compared to ML and HL groups, suggesting the metabolic flow of iridoid metabolites in *G. macrophylla* was prevented under low light. As a result, the content of loganic acid was significantly decreased, as well as the genes expression of *GmGES*, *GmG10H*, *Gm8-HGO*, *GmIS*, *Gm7-DLH* and *GmSLS*. However, the contents of gentiopicroside and sweroside were present higher in both LL and HL groups compared to ML group. It is difficult to explain the reason for the unrevealed pathway on biosynthesis of gentiopicroside, sweroside and swertiamarin. Considering the sharp decrease of loganic acid, we speculated that gentiopicroside might be the vital substance for the growth and development of *G. macrophylla*, thus, the metabolic flow from secologanate to gentiopicroside was abnormally activated at low light intensity.

The third consequence is that numerous physiological alterations such as changes in phytohormone levels, plant immune responses and signal-transduction pathways were induced in respond to the light stress in plants (Goh, et al. 2003; Taj, et al. 2010). As reported, the concentration of abscisic acid (ABA) were significantly increased under prolonged dark treatments of light-grown plants of both *Lemna gibba* and *Arabidopsis thaliana* (Weatherwax, et al. 1996). In addition, exogenous ABA was found to accelerate Chls breakdown and MDA accumulation, leading to leaves turn yellow easily (Xiao, et al. 2019). In our study, the expression of genes involved in the biosynthesis of ABA was upregulated by continuous exposure to low light (Supplementary Figs. 1 and 2, Supplementary Table 5). We speculated ABA played a vital role in respond to light stress in *G. macrophylla*. In addition, *trans*-zeatin as another major and ubiquitous cytokinin in higher plants (Veach, et al. 2003) can regulate external stimulus such as low light intensity and cold acclimation (Lee, et al. 2008; Prerostova, et al. 2021). Due to an increase expression at low light intensity, we speculated *trans*-zeatin was involved in response to light stress in *G. macrophylla*. Moreover, hormones were reported in response to light stress *via* MAPK signaling cascade (Sharma, et al. 2020). The genes related to pathogen infection, hydrogen peroxide signaling, as well as ethylene, jasmonic acid, and ABA hormone signaling pathways, along with the expression of genes related to wounding-related enzymes, were significantly changed after light treatment (Supplementary Figs. 7 and 8, Supplementary Table 8), suggesting that a series of MAPK signaling transductions were triggered in *G. macrophylla* leaves exposure to low or high light. In brief, a complex and extensive regulatory network would be performed to restore internal balance, when plants perceived various different light intensities.

The last consequence, TFs as essential regulators of the key enzyme genes in the secondary metabolite biosynthesis pathway, can be regulated by light (Huang, et al. 2022; Xie, et al. 2022; Zhang, et al. 2021). As reported, *CYP450s*, *MYB*, and *AP2/ERF* genes may be involved in paclitaxel biosynthesis and play an important role in excessive light in *Taxus chinensis* (Li, et al. 2022). In our research, the biosynthesis of loganic acid in *G. macrophylla* might be affected by *GmbHLH20* and *GmMYB5*, for the expression of genes in the iridoid synthesis pathway as *GmDXS*, *GmHDR*, *GmGES*, *GmG10H*, *Gm8-HGO*, *GmIS*, *GmIO*, *Gm7-DLH*, *GmGGPPS*, *GmHMGR* and *Gm7-DLNGT* showed high correlation with *GmbHLH20*, while the expression of *GmHMGR*, *GmG10H*, *Gm7-DLNGT*, and *Gm8-HGO* showed high correlation with *GmMYB5* (Fig. 9d). In addition, TFs might form complexes to regulate diverse metabolic and developmental processes in plants (Wang, et al. 2022). As a negative correlation was present, the regulatory mechanism of *GmbHLH20* and *GmMYB5* was deduced to be performed independently.

Conclusion

This study represented the first comprehensive investigation of mechanism of iridoid biosynthesis in *G. macrophylla* under different light intensities by transcriptome and metabolome. A model was proposed to explain the underlying molecular mechanism, as shown in Fig. 11. Initially, the rate of photosynthesis was primarily affected along with a decrease in light intensity, the contents of Chls and carotenoids exhibited lower expression as well as their biosynthesis genes, resulting in the seedlings gradually turning yellow and wilt. Subsequently, the alteration of photosynthesis regulated the primary metabolic system, the secondary metabolic pathway, the key responsive TFs and light related hormone signaling, finally affected the iridoid metabolites accumulation. It was a complex and extensive regulatory network, in which two TFs of *GmMYB5* and *GmbHLH20* were determined to play crucial roles in respond to light stress of iridoid metabolites production in *G. macrophylla*. Our research reveals the interplay between photosynthesis and iridoid biosynthesis in *G. macrophylla*, and helps us understand the potential mechanism of ecological factors modulating metabolite accumulation.

Abbreviations

LED light-emitting diodes

DEGs Differentially expressed genes

DMGs Differentially expressed metabolites

Chl Chlorophyll

ML Medium light

HL High light

LL Low light

TF Transcription factor

MEP Methyl-erythrose 4-phosphate pathway

MVA Mevalonate pathway

ABA Abscisic acid

MAPK Mitogen activated protein kinase

GO Gene ontology

KEGG Kyoto encyclopedia of genes and genomes

FDR False discovery rate

NCBI National center for biotechnology information

Nr Non-redundant

PPFD The photosynthetic photon flux density

RT-qPCR Quantitative reverse transcription PCR

Declarations

Funding

This study was supported by the Natural Science Foundation of China (No. 81903753), the Key Industry Innovation Chain (Group) of Shaanxi Province (No. 2023-ZDLSF-58), the Key Research and Development Program of Shaanxi Province (No. 2022SF-089), the Natural Science Foundation of Qinghai (No. 2022-ZJ-917), the Project on Collaborative Innovation of Shaanxi Provincial Department of Education (No. 21JY011, 23JY024), the Key Program (A) of Shaanxi Provincial Health Commission (No. 2021A008) and the Subject of Science Leader Team of the Shaanxi University of Chinese Medicine.

Competing Interests

All authors certify that they have no affiliations with or involvement in any organization or entity with any financial interest or non-financial interest in the subject matter or materials discussed in this manuscript.

Author Contributions

All authors contributed to the study conception and design. The experiment was designed by YZG and HYH, and conceived by FHH and WYM. Material preparation was performed by FHH, WYM and MFK. Data collection and analysis were performed by FHH, WYM, WL, YY and WF. The first draft of the

manuscript was written and revised by FHH, HYH and YZG and all authors commented on previous versions of the manuscript. All authors read and approved the final manuscript.

Data Availability

The data presented in the study are deposited in the NCBI repository with the link https://www.ncbi.nlm.nih.gov/. The accession number is PRJNA1043239.

Supplementary Information

The online version contains supplementary material available at https: //doi.org/10.1007/sxxxx-xxx-xxxxx-x.

References

1. Ahmad SN, Morteza K, Mortaza E, Kosar M, Poone B, Nafiseh N (2019) Effect of different quality of light on growth and production of secondary metabolites in adventitious root cultivation of *Hypericum perforatum*. Plant Signal & Behav 14:1559–2324. https://doi.org/10.1080/15592324.2019.1640561
2. Barh A, Chiocchio I, Barbaresi A, Barbanti L, Mandrone M, Poli F, Torreggiani D, Trenta M, Tassinari P (2022) Effects of LED supplemental lighting on the growth and metabolomic profile of *Taxus baccata* cultivated in a smart greenhouse. PLoS ONE 17:e0266777. https://doi.org/10.1371/journal.pone.0266777
3. Cao XY, Wang ZZ (2010) Simultaneous determination of four iridoid and secoiridoid glycosides and comparative analysis of Radix Gentianae Macrophyllae and their related substitutes by HPLC. Phytochem Anal 21:348–354. https://doi.org/10.1002/pca.1206
4. Chen IGJ, Lee MS, Lin MK, Ko CY, Chang WT (2018) Blue light decreases tanshinone IIA content in *Salvia miltiorrhiza* hairy roots via genes regulation. J Photochem Photobiol B-Biol 183:164–171. https://doi.org/10.1016/j.jphotobiol.2018.04.013
5. Gad G, Rachel A, Alisdair RF (2016) The regulation of essential amino acid synthesis and accumulation in plants. Annu Rev Plant Biol 67:153–178. https://doi.org/10.1146/annurev-arplant-043015-112213
6. Goh CH, Nam HG, Park YS (2003) Stress memory in plants: a negative regulation of stomatal response and transient induction of rd22 gene to light in abscisic acid-entrained *Arabidopsis* plants. Genes 36:240–255. https://doi.org/10.1046/j.1365-313X.2003.01872.x
7. Gong M, Jiang DZ, Liu R, Tian SM, Xing HT, Chen ZD, Shi RJ, Li HL (2023) Influence of high-temperature and intense light on the enzymatic antioxidant system in Ginger (*Zingiber officinale* Roscoe) plantlets. Metabolites 13:992. https://doi.org/10.3390/metabo13090992
8. Guo XL, Shakeel M, Wang DL, Qu CP, Yang SM, Ahmad S, Song ZJ (2022b) Metabolome and transcriptome profiling unveil the mechanisms of light-induced anthocyanin synthesis in rabbiteye

blueberry *(vaccinium ashei*: Reade). BMC Plant Biol 22:223. https://doi.org/10.1186/s12870-022-03585-x

9. Guo XZ, Li Q, Yan BB, Wang YF, Wang S, Xiong F, Zhang CC, Zhang Y, Guo LP (2022a) Mild shading promotes sesquiterpenoid synthesis and accumulation in *Atractylodes lancea* by regulating photosynthesis and phytohormones. Sci Rep 12:21648. https://doi.org/10.1038/s41598-022-25494-7
10. HÄDer DP (2022) Photosynthesis in plants and algae. Anticancer Res 42:5035–5041. https://doi.org/10.21873/anticanres.16012
11. Han ZH, An XL, Tan TY, Song ZJ, Guo XL, Zhang XY, Zhu YZ, Wang DL (2023) Physiological response of anthocyanin synthesis to different light intensities in blueberry. PLoS ONE 18:e0283284. https://doi.org/10.1371/journal.pone.0283284
12. Hao ZY, Wang XL, Yang M, Cao B, Zeng MN, Zhou SQ, Li M, Cao YG, Xie SS, Zheng XK, Feng WS (2023) Minor iridoid glycosides from the fruits of *Cornus officinalis* Sieb. et Zucc. and their anti-diabetic bioactivities. Phytochemistry 205:113505. https://doi.org/10.1016/j.phytochem.2022.113505
13. He YH, Yan HL, Hua WP, Huang YY, Wang ZZ (2016) Selection and validation of reference genes for quantitative real-time PCR in *Gentiana macrophylla*. Front Plant Sci 07:945. https://doi.org/10.3389/fpls.2016.00945
14. Hu W, He YH, Yin YY, Yang Y, Fu HH, Li Z, Yue ZG (2022) Three rare furan derivatives transformed from secoiridoids were isolated from the roots of *Gentiana macrophylla*. Rec Nat Prod 16:651–656. https://doi.org/http://doi.org/10.25135/rnp.322.2201.2333
15. Huang YJ, Zhai YN, Huang Y, Huang YF, Liu K, Zhang J, Zhou JH (2022) Effects of light intensity on physiological characteristics and expression of genes in coumarin biosynthetic pathway of *Angelica dahurica*. Int J Mol Sci 23:15912. https://doi.org/10.3390/ijms232415912
16. Kc S, Long LZ, Liu MY, Zhang QF, Ruan JY (2021) Light intensity modulates the effect of phosphate limitation on carbohydrates, amino acids, and catechins in tea plants (*Camellia sinensis* L). Front Plant Sci 12:743781. https://doi.org/10.3389/fpls.2021.743781
17. Kim D, Langmead B, Salzberg SL (2015) HISAT: a fast spliced aligner with low memory requirements. Nat Methods 12:357–360. https://doi.org/10.1038/nmeth.3317
18. Lee SG, Ko KD, Lee C (2008) Influence of post-fruit set plant exposure to low light intensity on growth and yield of oriental melon. Acta Hortic 771:249–255. https://doi.org/10.17660/ActaHortic.2008.771.37
19. Li JH, Zeng R, Li WT, Huang LF (2016) Correlation analysis between quality of *Gentiana macrophylla* Pall. and climatic factors. Word Chin Med 5:801–806. https://doi.org/10.3969/j.issn.1673-7202.2016.01.011
20. Li TT, Li BB, Liao CL, Zhang HM, Wang LZ, Fu TT, Xue SY, Sun T, Xu XL, Fan X, Li L, Liu GL, Yang FL, Ma X (2022) Transcriptome analysis provides insights into light condition effect on paclitaxel biosynthesis in yew saplings. BMC Plant Biol 22:577. https://doi.org/10.1186/s12870-022-03958-2

21. Liu ZH, Meng LJ, Wang MK, Wang L, Liu YH, Hou GX, Li SM, Kang WY (2023) New iridoids from *Patrinia scabiosaefolia* and their hypoglycemic effects by activating PI3K/Akt signaling pathway. Fitoterapia 165:105423. https://doi.org/10.1016/j.fitote.2022.105423
22. Love MI, Huber W, Anders S (2014) Moderated estimation of fold change and dispersion for RNA-seq data with DESeq2. Genome Biol 15:550. https://doi.org/10.1186/s13059-014-0550-8
23. Lu YY, Zhang XB, Yang YM, MA XH, Zhu TT, Yu XH, Jin L (2016) Quality regionalization study on Gentianae Macrophyllae Radix. China J Chin Mater Med 41. https://doi.org/10.4268/cjcmm20161704
24. Peng MC, Ai XH (2021) Research progress in chemical constituents, pharmacological effects and clinical application of the flowers of *Gentianae Macrophylla*. Cent S Pharm 19:1243–1249. https://doi.org/10.7539/j.issn.1672-2981.2021.06.039
25. Prerostova S, Dobrev PI, Knirsch V, Jarosova J, Gaudinova A, Zupkova B, Prášil IT, Janda T, Brzobohatý B, Skalák J, Vankova R (2021) Light quality and intensity modulate cold acclimation in *Arabidopsis*. Int J Mol Sci 22:2736. https://doi.org/10.3390/ijms22052736
26. Proietti S, Paradiso R, Moscatello S, Saccardo F, Battistelli A (2023) Light Intensity affects the assimilation rate and carbohydrates partitioning in spinach grown in a controlled environment. Plants 12:804. https://doi.org/10.3390/plants12040804
27. Shang J, Zhao LP, Yang XM, Qi XL, Yu JF, Du JB, Li K, He CS, Wang WM, Yang WY (2023) Soybean balanced the growth and defense in response to SMV infection under different light intensities. Front Plant Sci 14:1150870. https://doi.org/10.3389/fpls.2023.1150870
28. Shao DN, Zhu QH, Liang Q, Wang XF, Li YJ, Sun YQ, Zhang XY, Liu F, Xue F, Sun J (2022) Transcriptome analysis reveals differences in anthocyanin accumulation in Cotton (*Gossypium hirsutum* L.) induced by red and blue light. Front Plant Sci 13:788828. https://doi.org/10.3389/fpls.2022.788828
29. Sharma D, Verma N, Pandey C, Verma D, Bhagat PK, Noryang S, Singh K, Tayyeba S, Banerjee G, Sinha AK (2020) MAP Kinase as regulators for stress responses in plants. In: Prot Kinases Stress Signal Plants. G.K. Pandey (Ed.). pp 369–392
30. Shi Z, Deng XX, Zeng LX, Shi SQ, Lei L, Xiao WF (2022) Acclimation strategy of Masson Pine (*Pinus massoniana*) by limiting flavonoid and terpenoid production under low light and drought. Int J Mol Sci 23:8441. https://doi.org/10.3390/ijms23158441
31. Taj G, Agarwal P, Grant M, Kumar A (2010) MAPK machinery in plants: Recognition and response to different stresses through multiple signal transduction pathways. Plant Signal Behav 5:1370–1378. https://doi.org/10.4161/psb.5.11.13020
32. Usmanov D, Azamatov A, Baykuziyev T, Yusupova U, Rasulev B (2023) Chemical constituents, anti-inflammatory and analgesic activities of iridoids preparation from *Phlomoides labiosa* bunge. Nat Prod Res 37:1709–1713. https://doi.org/10.1080/14786419.2022.2104274
33. Veach YK, Martin RC, Mok DWS, Malbeck J, Vankova R, Mok MC (2003) O-glucosylation of cis-zeatin in maize. characterization of genes, enzymes, and endogenous cytokinins. Plant Physiol 131:1374–

1380. https://doi.org/10.1104/pp.017210

34. Wang BH, Luo Q, Li YP, Du KX, Wu Z, Li TY, Shen WH, Huang CH, Gan JH, Dong AW (2022) Structural insights into partner selection for MYB and bHLH transcription factor complexes. Nat Plants 8:1108–1117. https://doi.org/10.1038/s41477-022-01223-w
35. Weatherwax SC, Ong MS, Degenhardt J, Bray EA, Tobin EM (1996) The interaction of light and abscisic acid in the regulation of plant gene expression. Plant physiol 111:363–370. https://doi.org/10.1104/pp.111.2.363
36. Wen B, Mei ZL, Zeng CW, Liu SQ (2017) MetaX: a flexible and comprehensive software for processing metabolomics data. BMC Bioinform 18:183. https://doi.org/10.1186/s12859-017-1579-y
37. Wu LH, Ye Y, Li XS, Duan CH, Wang ZT (2009) RP-HPLC determ ination of gentiopcroside in Radix Gentianae Macrophyllae in tranditional area. Chin J Pham Anal 29:184–187
38. Xiao HJ, Liu KK, Ma YB, Gong ZH (2019) Physiological and biochemical changes during leaf senescence under the regulation of exogenous ABA in *Capsicum annuum* L. J Henan Agr University 53:357–364. https://doi.org/10.16445/j.cnki.1000-2340.2019.03.006
39. Xie GW, Zou XZ, Liang ZH, Wu D, He JK, Xie KC, Jin HL, Wang HB, Shen Q (2022) Integrated metabolomic and transcriptomic analyses reveal molecular response of anthocyanins biosynthesis in perilla to light intensity. Front Plant Sci 13:976449. https://doi.org/10.3389/fpls.2022.976449
40. Yang YY, Zhang X, Han MZ, Hu ZH, Wu J, Ma N, Leng PS, Zhou XF (2023) LiMYB108 is involved in floral monoterpene biosynthesis induced by light intensity in *Lilium 'Siberia'*. Plant Cell Rep 42:763–773. https://doi.org/10.1007/s00299-023-02995-x
41. Yoon YE, Cho JY, Kim YN, Kantharaj V, Lee KA, Seo WD, Lee YB (2023) Variation of saponarin content in Barley Sprouts (*Hordeum vulgare* L.) by natural light shielding: implication of the importance of light intensity. ACS Omega 8:35837–35844. https://doi.org/10.1021/acsomega.3c03458
42. Yoshikawa H, Matsumoto T, Kitagawa T, Okayama M, Ohta T, Yoshida T, Watanabe T (2022) Anti-proliferative effects of iridoids from *Valeriana fauriei* on cancer stem cells. Int J Mol Sci 23:14206. https://doi.org/10.3390/ijms232214206
43. Zengin G, El-Raey M, El-Kashak W, Batiha GE-S, Althumairy D, Alamer S, Mostafa NM, Eldahshan OA (2023) Sweroside: An iridoid glycoside of potential neuroprotective, antidiabetic, and antioxidant activities supported by molecular docking. Amino Acids 55:1765–1774. https://doi.org/10.1007/s00726-023-03262-9
44. Zhang QF, Liu MY, Ruan JY (2017) Integrated transcriptome and metabolic analyses reveals novel insights into free amino acid metabolism in huangjinya tea cultivar. Front Plant Sci 8:291. https://doi.org/10.3389/fpls.2017.00291
45. Zhang SC, Zhang L, Zou HY, Qiu L, Zheng YW, Yang DF, Wang YP (2021) Effects of light on secondary metabolite biosynthesis in medicinal plants. Front Plant Sci 12:781236. https://doi.org/10.3389/fpls.2021.781236
46. Zhang X, Su XY, Yu XY, Zhang XY, Guo XL, Hou GG, Wang CH, Li HJ (2023) Preparative separation of iridoid glucosides and crocins from *Gardeniae Fructus* using sequential macroporous resin column

chromatography and evaluation of their anti-inflammatory and antioxidant activities. J Chromatogr 1229:123887. https://doi.org/10.1016/j.jchromb.2023.123887

47. Zhao QZ, Dong MY, Li MF, Jin L, Paré PW (2023) Light-induced flavonoid biosynthesis in *Sinopodophyllum hexandrum* with high-altitude adaptation. Plants 12:575. https://doi.org/10.3390/plants12030575
48. Zhou B, Feng X, Huang W, Liu Q, Ibrahim SA, Liu Y (2023) Effects of light intensity on the biosynthesis of glucosinolate in Chinese cabbage plantlets. Sci Hortic 316:112036. https://doi.org/10.1016/j.scienta.2023.112036
49. Zhou T, Bai GQ, Hu YH, Ruhsam M, Yang YC, Zhao YM (2022) De novo genome assembly of the medicinal plant *Gentiana macrophylla* provides insights into the genomic evolution and biosynthesis of iridoids. DNA Res 29:1–15. https://doi.org/10.1093/dnares/dsac034

Figures

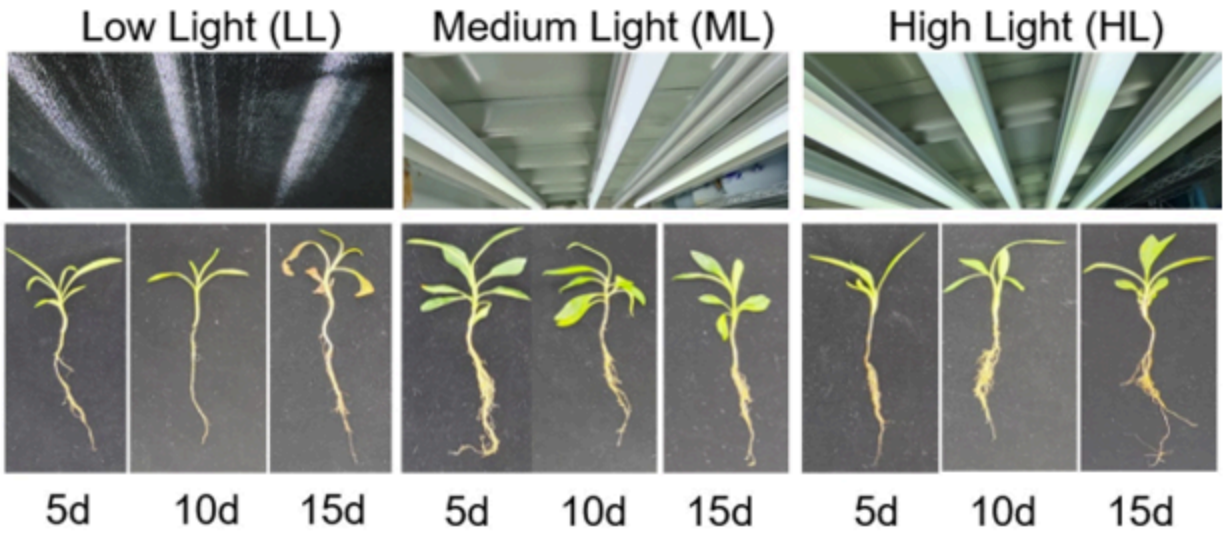


Figure 1

The growth conditions of *G. macrophylla* seedlings under different light intensity treatments at the 5th, 10th and 15th day, respectively. LL, ML and HL indicates under low, medium and high light treatment group, respectively

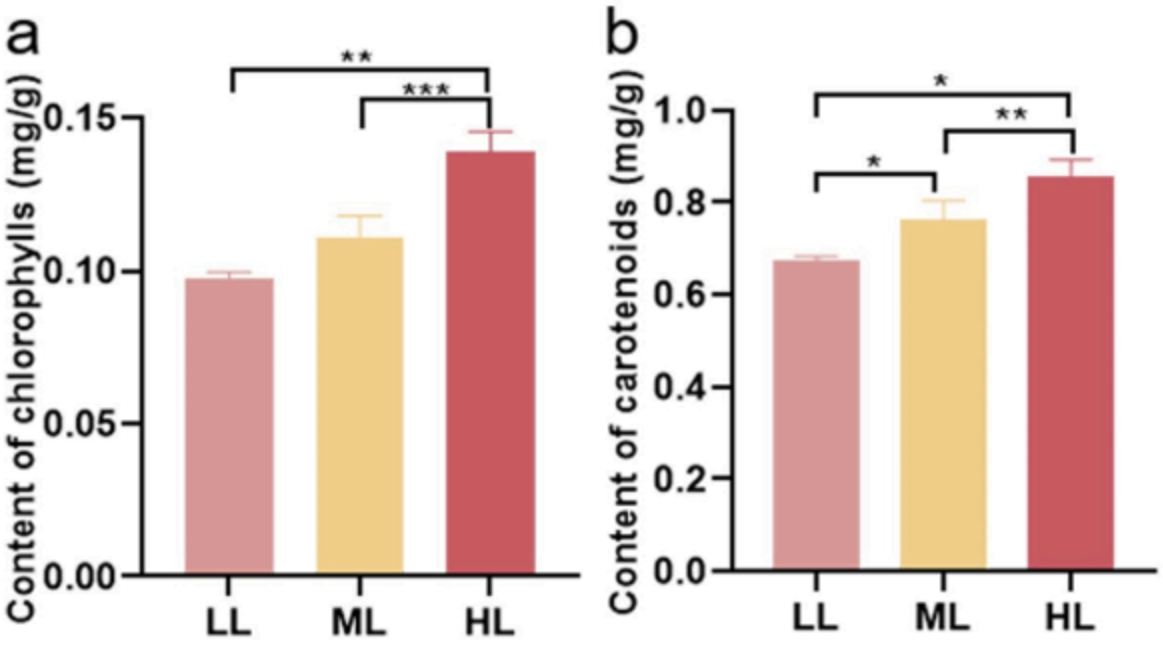


Figure 2

The contents of chlorophylls and carotenoids under different light intensity treatments at 5-day in *G. macrophylla* seedlings leaves. (a) Chlorophyllscontent. (b) Carotenoids content. *Statistically significant differences (* P< 0.05, ** P < 0.01, and *** P < 0.001)

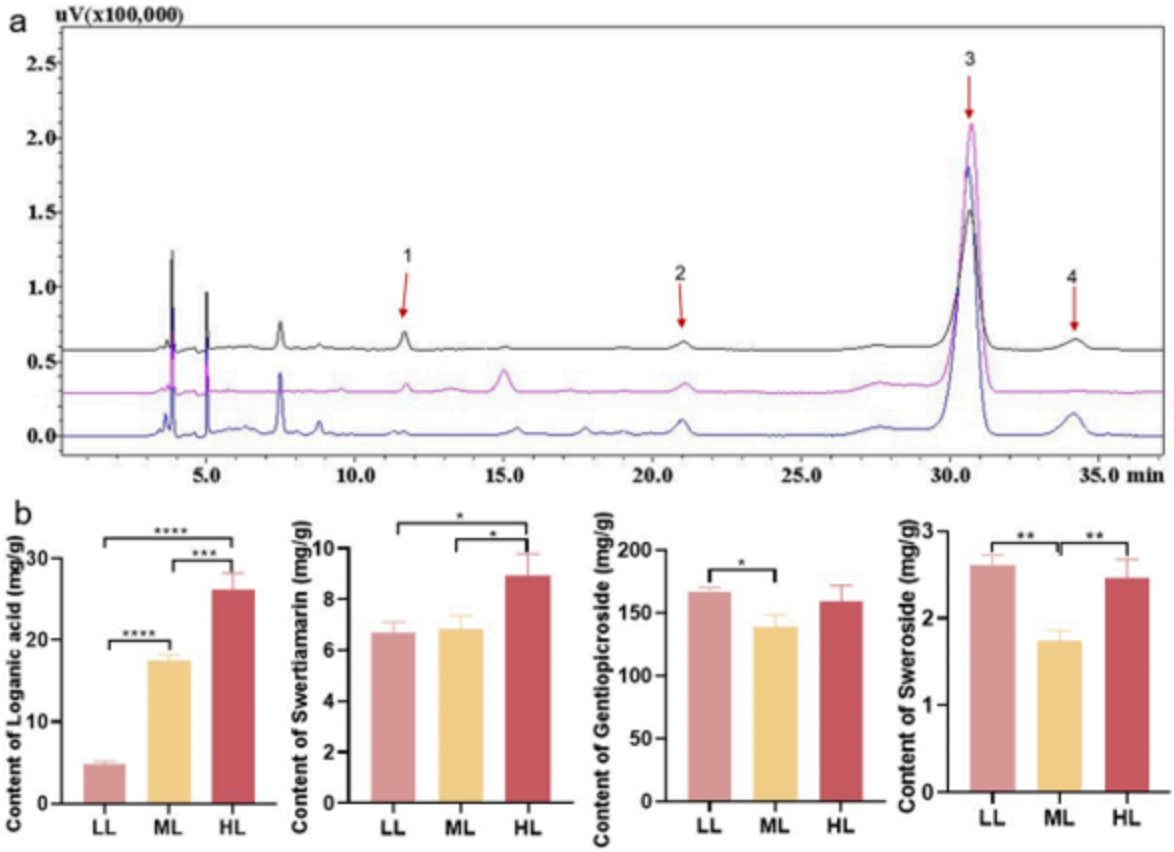


Figure 3

HPLC contents determination of four major iridoid metabolites at 5-day. (a) Black, pink, and blue represents chromatogram of ML, LL, and HL, while, 1, 2, 3 and 4 represents chromatographic peak of loganic acid, swertiamarin, gentiopicroside and sweroside, respectively. (b) The contents determination of four major iridoid metabolites.*Statistically significant differences (* $P < 0.05$, ** $P < 0.01$, *** $P < 0.001$, and **** $P < 0.0001$)

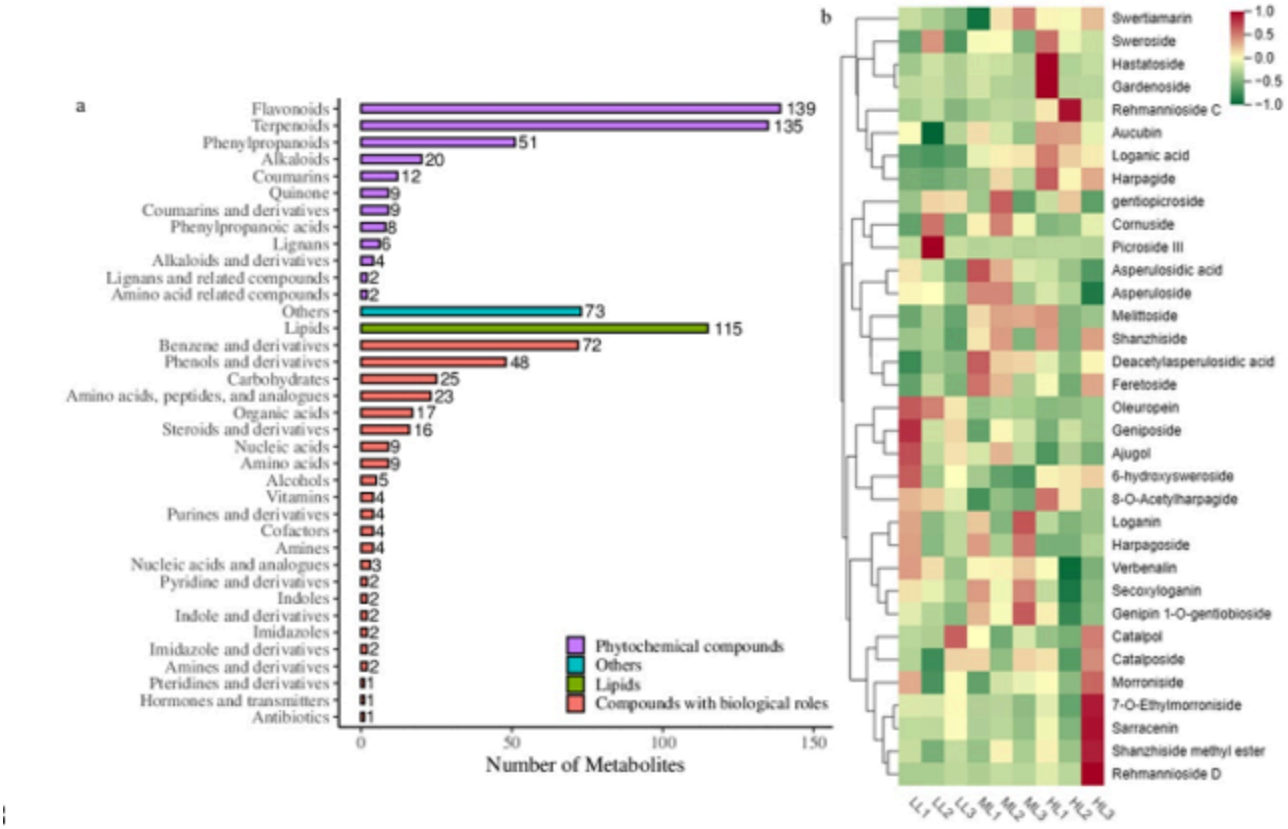


Figure 4

Untargeted metabolome analysis of metabolic composition in *G. macrophylla* seedlings leaves treated with different light intensities at 5-day. (a) Bar diagram depicts metabolites classification. The x-axis and y-axis represent the numbers and the classes of metabolites, respectively. (b) Hierarchical clustering heatmap analysis of iridoid compounds by z-score. Color represents the scale of iridoids contents. Red indicates upregulation, while, green indicates downregulation

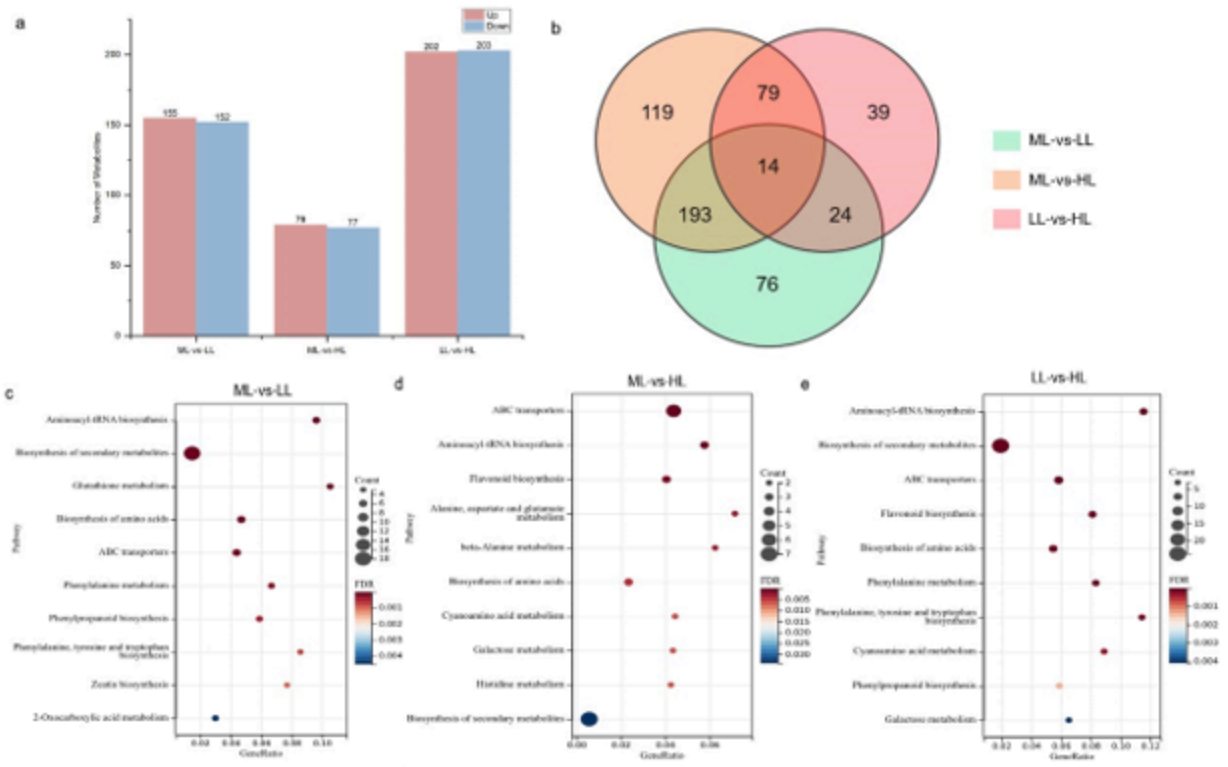


Figure 5

Untargeted metabolome analysis of differentially expressed metabolites (DEMs) in the ML-*vs*-LL, ML-*vs*-HL, and LL-*vs*-HL comparisons at 5-day. (a) Numbers of DEMs. Red indicates upregulation, while, blue indicates downregulation. (b) Venn diagram depicting the numbers of shared and specific metabolites in the three compared groups. (c-e) KEGG enrichment analysis of the DEMs

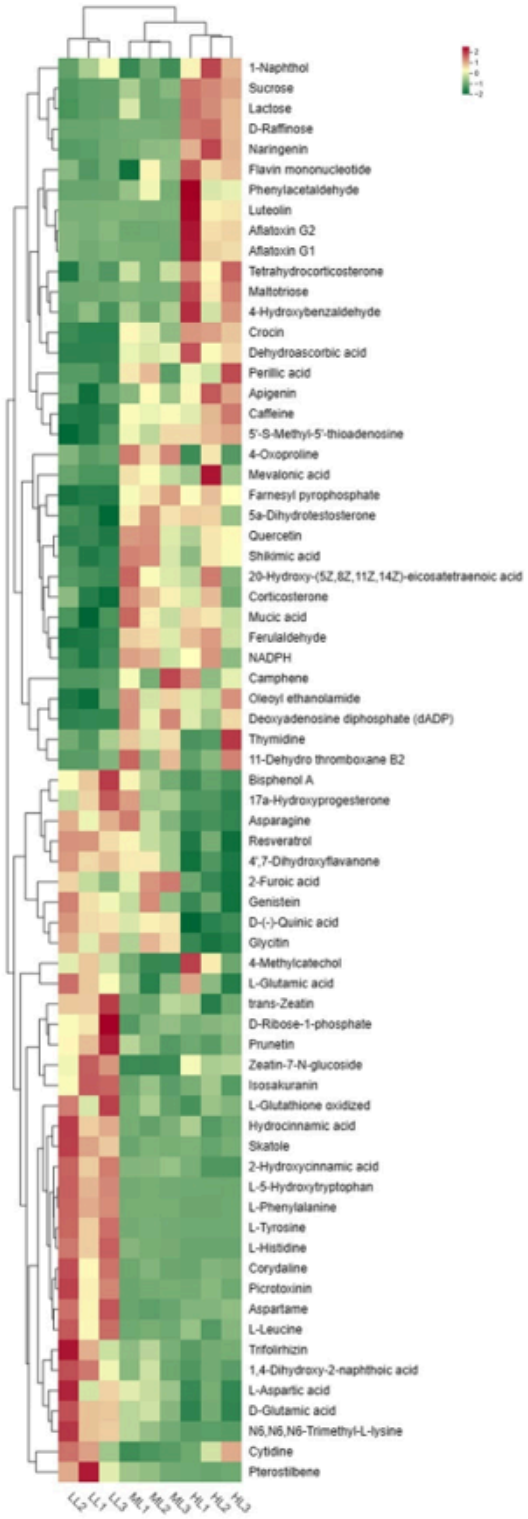


Figure 6

The contents of the 70 identified DEGs refer to KEGG pathway. The color represents the scale of iridoids contents. Red indicates upregulation, while, green indicates downregulation

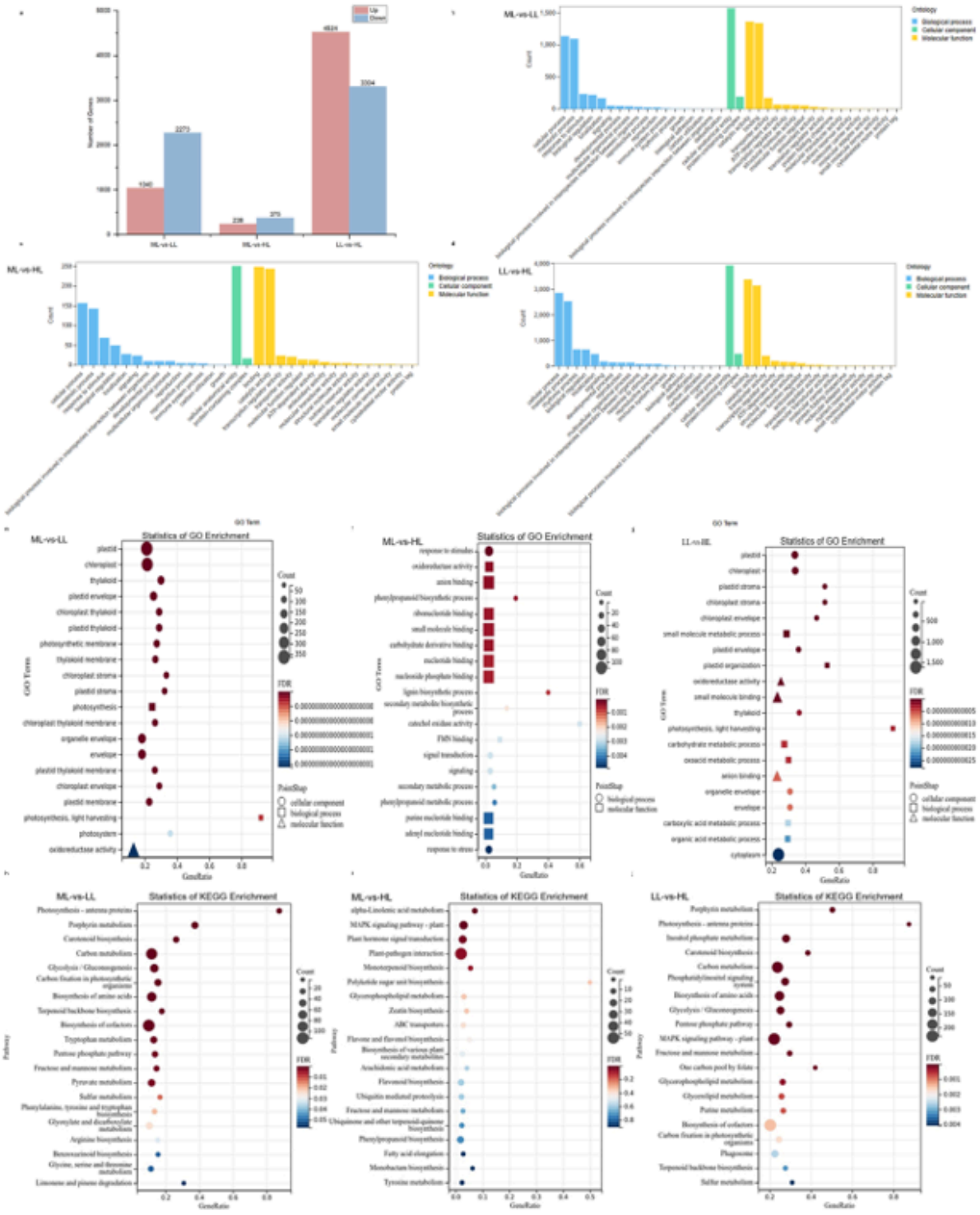


Figure 7

Differentially expressed genes (DEGs) analysis in the ML-*vs*-LL, ML-*vs*-HL, and LL-*vs*-HL comparisons at 5-day. (a) Numbers of DEGs. Red indicates upregulation, while, blue indicates downregulation. (b-d) Bar diagrams of GO classifications of DEGs. (e-g) GO enrichment analysis of the DEGs. (h-j) KEGG enrichment analysis of the DEGs

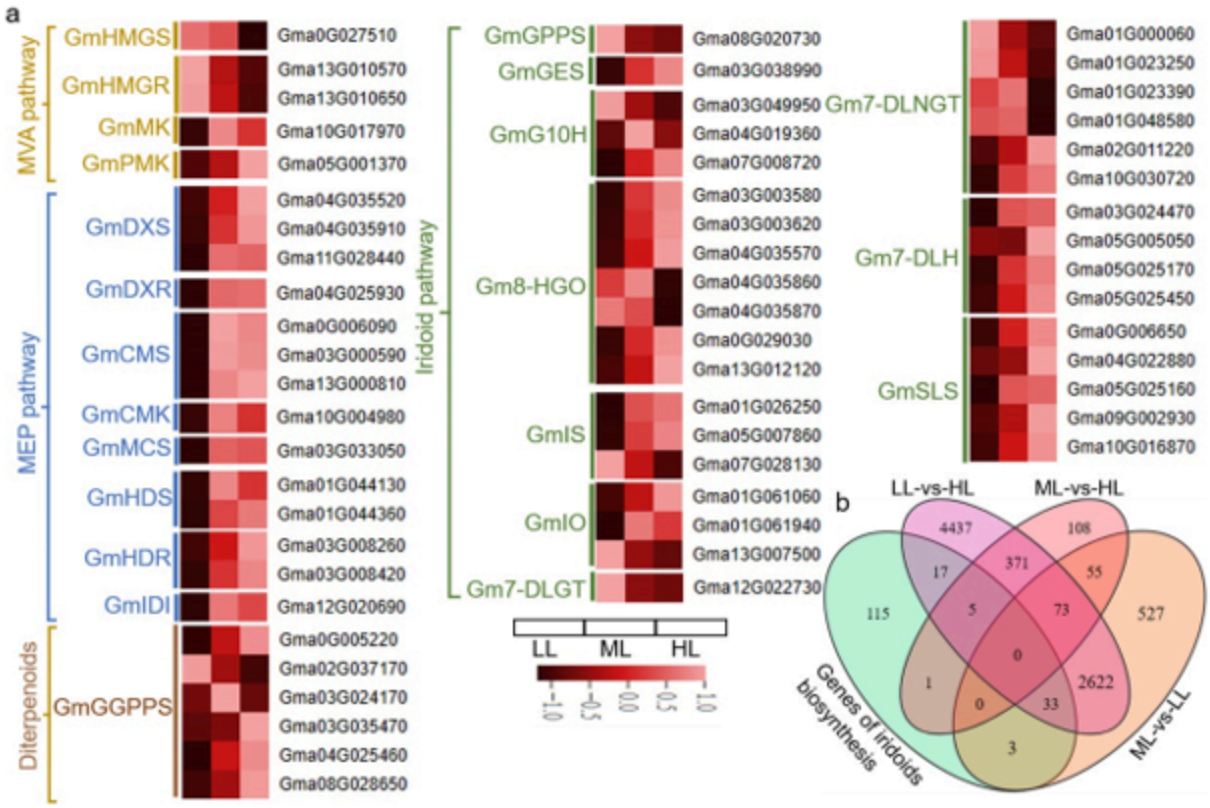


Figure 8

The expression of DEGs involved in iridoid biosynthesis at 5-day. (a) Heatmap of DEGs expression levels (normalized *via z*-score). Color shade represents expression levels. (b) Venn diagram depicting comparison of the DEGs numbers in the iridoid biosynthesis pathway

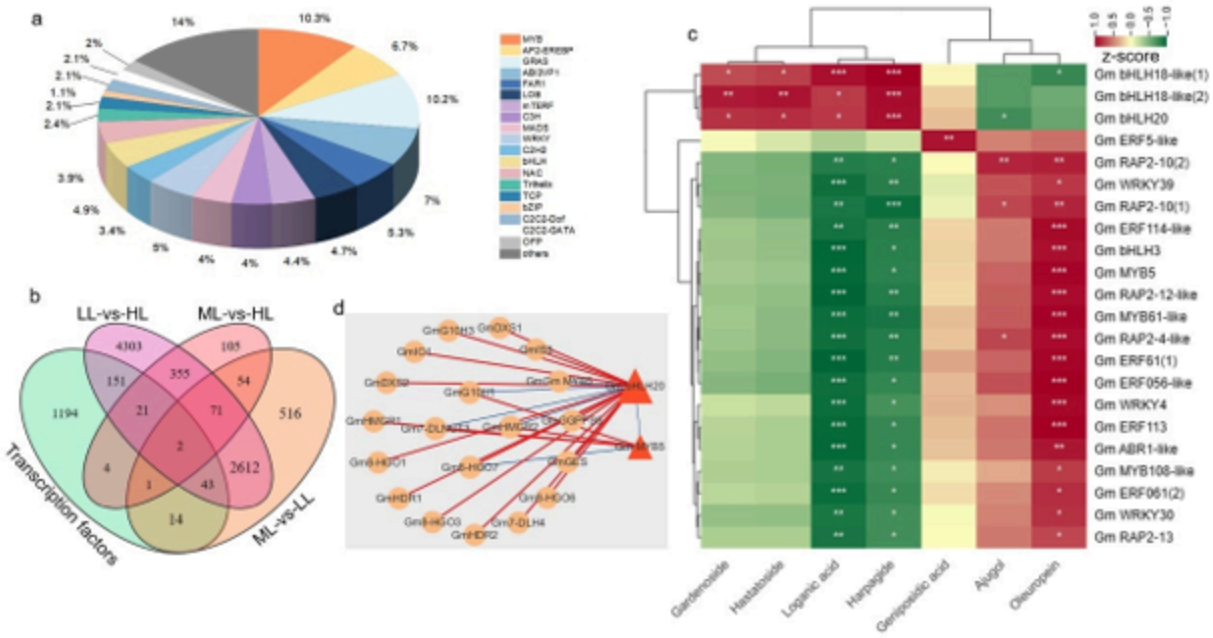


Figure 9

Analysis of transcription factors (TFs). (a) Distribution of TFs. (b) Venn diagram depicting comparison of the differential TFs numbers. (c) Heatmap of correlation between differential TFs and iridoid compounds, $R \geq 0.8$. (d) Correlation network diagram among the DEGs in iridoids biosynthesis, *GmbHLH20* and *GmMYB5*, $R \geq 0.8$. Red lines indicate a positive correlation, while blue lines indicate a negative correlation and line thickness indicates the strength of the correlation

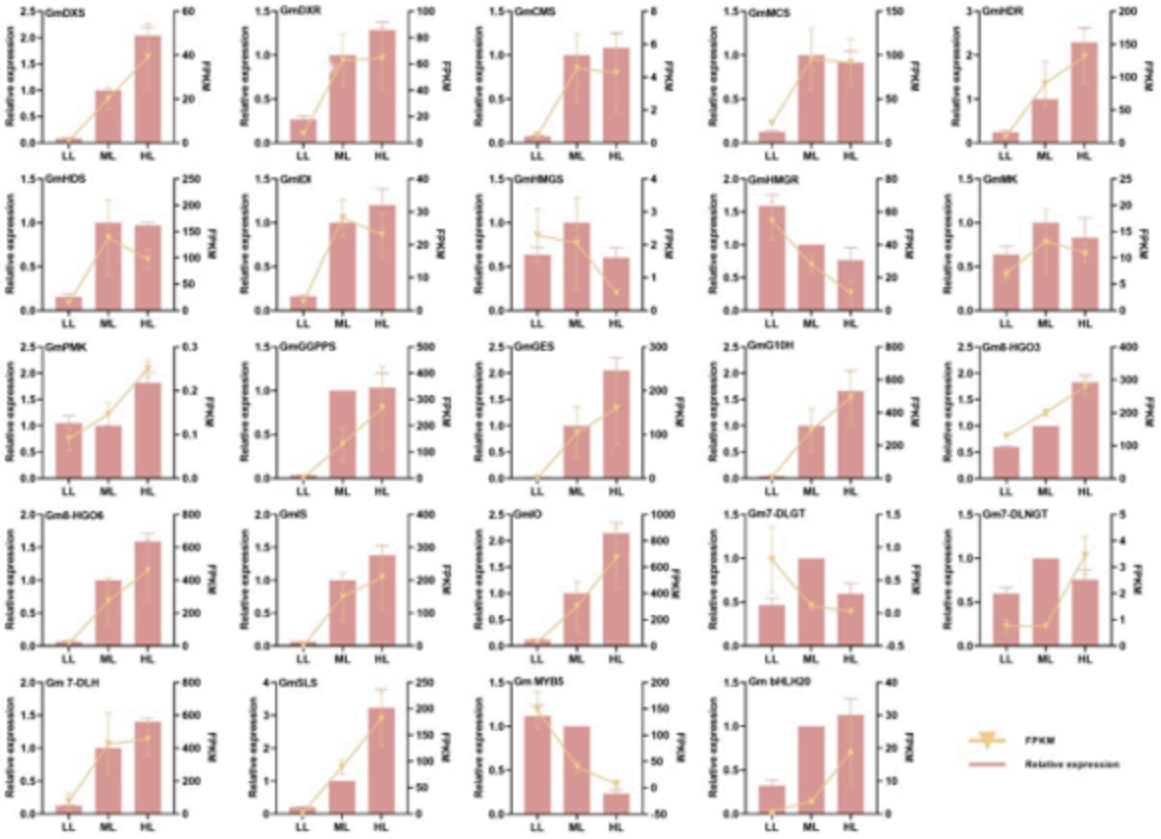


Figure 10

Determination of selected DEGs expression via RNA-seq and RT-qPCR. The x-axis, left y-axis and right y-axis indicates the three treatment groups, RT-qPCR expression levels and the RNA-seq data with FPKM, respectively. Error bars indicate the standard deviation of three independent replicates

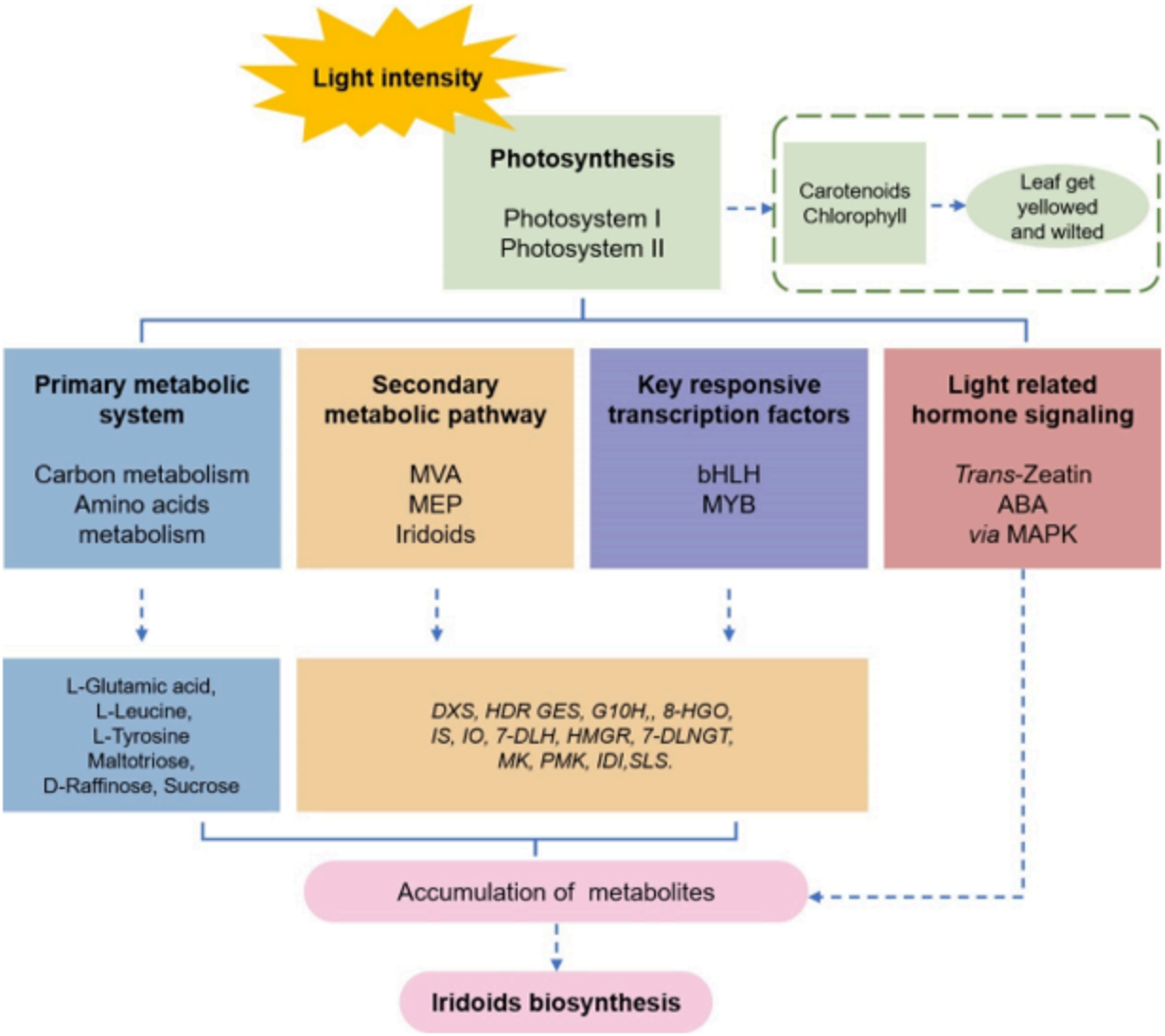


Figure 11

A schematic overview: working model of light regulation on iridoids biosynthesis in *G. macrophylla*

Supplementary Files

This is a list of supplementary files associated with this preprint. Click to download.

- SupplementaryInformationofFigures.docx
- SupplementaryInformationofTables.xlsx